Published in final edited form as:
Cancer Res. 2011 September 15; 71(18): 6010–6018. doi:10.1158/0008-5472.CAN-11-0595.

Activated NOTCH1 induces lung adenomas in mice and cooperates with MYC in the generation of lung adenocarcinoma

Thaddeus D. Allen[1,3], **Elena M. Rodriguez**[1], **Kirk D. Jones**[2], and **J. Michael Bishop**[1]

[1]G.W. Hooper Research Foundation, University of California, San Francisco

[2]Department of Pathology and Laboratory Medicine, University of California, San Francisco

Abstract

NOTCH1 encodes the canonical member of the mammalian Notch receptor family. Activating lesions frequently affect *NOTCH1* in T-cell acute lymphoblastic leukemia (T-ALL) and recently have been found in non-small cell lung cancer (NSCLC) as well. We explored the oncogenic potential of activated NOTCH1 in the lung by developing a transgenic mouse model in which activated NOTCH1 was overexpressed in the alveolar epithelium. The initial response to activated NOTCH1 was proliferation and the accumulation of alveolar hyperplasia, which was then promptly cleared by apoptosis. After an extended latency period, however, pulmonary adenomas arose in the transgenic mice, but failed to progress to carcinoma. Interestingly, MYC and MYCL1 were expressed in the adenomas, suggesting that selection for enhanced MYC activity may facilitate tumorigenesis. Using mice engineered to co-express activated NOTCH1 and MYC, we found that supplementing MYC expression increased the frequency of N1ICD-induced adenomas and enabled progression to adenocarcinoma and metastases. Cooperation stemmed from synergistic activation of tumor cell cycling, a process that apparently countered any impedance to tumorigenesis posed by MYC and/or activated NOTCH1-induced apoptosis. Significantly, cooperation was independent of RAS activation. Taken together, the data suggest that activated NOTCH1 substitutes for RAS activation in cooperation with MYC in the development of NSCLC. These tumor models should be valuable for exploring the role of activated NOTCH1 in the genesis of NSCLC and for testing therapies targeting either activated NOTCH1 or its downstream effectors.

Introduction

The Notch signaling pathway functions in cell-fate determination and differentiation (1). There are four *NOTCH* genes in the mammalian genome (*NOTCH1-4* in humans). The genes encode single pass transmembrane proteins that interact with ligands of the Delta and/or Jagged/Serrate family. The ligands are also transmembrane proteins, which bind to Notch receptors displayed on adjacent cells. Ligand binding induces proteolytic cleavage of the Notch receptor and release of the Notch intracellular domain (NICD) (2, 3). This is the activated form of NOTCH, which enters the nucleus and functions as a transcriptional co-activator for DNA-binding transcription factors of the CBF1/SU(H)/LAG1 (CSL) family (4). Notch target genes are normally repressed by CSL family proteins, but become activated through the binding of a NICD/CSL complex and its recruitment of chromatin remodeling proteins (5).

[3]Correspondence: Thaddeus D. Allen, University of California, San Francisco, 513 Parnassus Avenue, HSW 1501, San Francisco, CA, U.S.A., 94143-0552, Thaddeus.Allen@ucsf.edu, Ph. 415-476-5350, Fx. 415-476-6185.

Conflicts of interest: None

A role for Notch signaling in cancer was first suspected with the characterization of t(7;9)(q34;q34.3) chromosomal translocations in a subset of human T-ALLs (6). The translocation breakpoints occur in an intron of the *NOTCH1* gene and result in the formation of an mRNA encoding a truncated and constitutively active NOTCH1 intracellular domain (N1ICD) protein fragment. It is now known that point mutations and small, frame shifting insertions or deletions in *NOTCH1* also occur in T-ALL (7). These alterations enable either ligand-independent cleavage and N1ICD release or interrupt the domain that regulates N1ICD turnover, the C-terminal PEST domain, resulting in N1ICD stabilization and sustained NOTCH1 signaling. It has been suggested that *NOTCH* alterations are uncommon in malignancies other than T-ALL (8), but activating alterations in *NOTCH1* have been described in approximately 10% of human NSCLCs (9). An additional 30% of NSCLCs have lost expression of NUMB, a negative regulator of NOTCH, resulting in increased NOTCH activity (9).

In order to explore the tumorigenic potential of activated NOTCH1, we targeted expression of a N1ICD transgene to the pulmonary epithelium. Expression of the transgene could be induced by administration of doxycycline (DOX). Continuous N1ICD overexpression in the alveolar epithelium induced lung adenomas, but not adenocarcinomas. Progression of lung adenomas overexpressing N1ICD to adenocarcinoma could be brought about by the additional overexpression of MYC, which cooperated with N1ICD through synergistic effects on tumor cell proliferation. Previously, activating mutations in *Kras* were found in tumors from a murine model of NSCLC that overexpresses MYC (10). The cooperation we observed between N1ICD and MYC was independent of RAS activation, suggesting that activated NOTCH1 can substitute for activated RAS in tumorigenesis with MYC. Our results authenticate the tumorigenic potential of activated NOTCH1 in the lung, particularly in combination with MYC, and raise the possibility that therapeutics targeting NOTCH1 may prove valuable in the treatment of human NSCLCs that express activated forms of the protein.

Materials and Methods

Genetically modified mice

Experimentation was conducted with the approval of the Institutional Animal Care and Use Committee (IACUC) of the University of California, San Francisco. Mice expressing the DOX-responsive reverse tetracycline transactivator (rtTA) under the control of the rat Clara cell secretory protein (CCSP) promoter (11) and mice that have a tetracycline-responsive promoter element that controls the transcription of human *N1ICD* (12) have both been previously described. Transgenic mice with a tetracycline-responsive promoter element that controls the transcription of the human *MYC* sequence were developed in this laboratory (13). A diet supplemented with DOX (200 mg/kg) was used to stimulate the transactivating function of the rtTA protein. Lung phenotypes were evaluated according to criteria recommended by the Mouse Models of Human Cancer Consortium (14). Under these recommendations adenocarcinomas are defined as tumors ≥ 5 mm in diameter, while adenoma, considered the precursor to adenocarcinoma, is < 5 mm in diameter.

Western analysis

Snap frozen lung and tumor tissues were used to prepare protein lysates and Western analysis was carried out using standard techniques. Sources of antibodies used for detection are listed in Supplementary Materials and Methods.

Tissue staining

Immunohistochemical staining was carried out using the Vector Elite ABC Kit (Vector Laboratories). Primary antibodies used for staining are listed in Supplementary Materials and Methods. We used the ApopTag® Peroxidase *In Situ* Apoptosis Detection Kit (Chemicon) for TUNEL staining. For the quantification of cells positive for phosphorylation of HISTONE 3 at Serine 10 (phospho-H3S10), Ki67 or TUNEL staining, at least three random high-powered fields were counted for each individual lung or tumor ($n \geq 3$ mice for each genotype).

Taqman analysis

RNA was extracted using the Absolutely RNA® Miniprep kit (Stratagene). RNA was reverse-transcribed using Stratascript reverse transcriptase (Stratagene) and analyzed by realtime-PCR (Taqman®, Applied Biosystems). Relative gene expression was normalized to a mouse *β-Actin* Taqman® probe using the ΔC_T method ($n \geq 3$ mice for each analysis).

RAS Activity Assay

RAS activity was measured in 250 μg of protein lysate using a RAS Activation Assay Kit (Millipore). In brief, the kit supplied a GST-RAF RAS-binding domain fusion protein to precipitate only ATP-bound RAS from protein lysate.

Results

Conditional expression of activated NOTCH1 in the alveolar epithelium

To model NOTCH1 activation in the lungs of adult mice we overexpressed N1ICD using a DOX-inducible system (Figure 1A). Transgenic mice expressing rtTA under the transcriptional control of the rat CCSP promoter (the C transgene) were used to achieve lung-specific expression. Although CCSP is expressed in Clara cells of the bronchiolar epithelium, the C transgene is transcriptionally active mainly in epithelial cells of the distal lung (11). We bred C mice to mice carrying a transgene encoding N1ICD (sequence of human *NOTCH1* encoding amino acids 1756–2556) under the transcriptional control of a tetracycline-response element (TRE) promoter (the N1 transgene) (12).

A diet supplemented with DOX was used to stimulate the transactivating function of the rtTA protein and induce N1ICD expression in the resulting CN1 mice. The 110 kDa N1ICD protein fragment was induced in CN1 mouse lungs after 7 continuous days of DOX treatment and reached a maximum level of expression after 14 days (Figure 1B). N1ICD levels decreased after day 14 but nonetheless remained elevated (see day 30, Figure 1B). We assayed the mRNA levels of a subset of known targets of the NOTCH transcriptional complex. Some responded to DOX induction, including *Hes5* and *Nrarp* (Figure 1C). Notably, *Hes1*, a gene whose transcription is often used as a measure of NOTCH activation, was not induced. Therefore, N1ICD overexpression activated only a subset of the known NOTCH targets, presumably reflecting tissue specific differences in the transcriptional program activated by NOTCH.

N1ICD induction of alveolar hyperplasia and apoptosis

We wished to assess if there were any acute consequences associated with N1ICD overexpression. Histological examination of H&E stained sections revealed an abundance of alveolar hyperplasia after 7 days of DOX treatment (compare Figure 1D with 1E). The hyperplasia was comprised of clusters of cells found in the alveolar space, reached a maximum after 14 days of DOX treatment (Figure 1F) and then regressed (Figure 1G). Regression was never absolute as hyperplastic cells persisted in the lungs of older mice

(compare Figure 1D with 1G). Immunohistochemical staining for NOTCH1 confirmed that the hyperplastic cells overexpressed N1ICD (Figure 1H–K).

We supposed that the transient hyperplasia could result from proliferation followed by apoptosis. Immunohistochemical staining for Ki67 antigen was performed to mark cycling cells (Supplementary Figure 1A–D). The number of cycling cells in DOX treated CN1 mice was substantially increased after 7 and 14 days of treatment, but regressed by 30 days of continuous DOX treatment (Figure 2A). TUNEL staining was used to detect apoptotic cells with fragmented DNA (Supplementary Figure 1E–H). CN1 mice did not have a substantial increase in $TUNEL^+$ cells after 7 days of continuous DOX treatment, but positive cells were abundant after 14 days and remained elevated after 30 days (Figure 2B). Therefore, alveolar epithelial cells proliferated in response to N1ICD overexpression, but cell death tempered the proliferative response.

N1ICD overexpression engages the BCL2 family of apoptotic regulators

To define mediators of the apoptosis that cleared N1ICD-induced alveolar hyperplasia, we screened protein lysates from DOX treated CN1 mice for alterations in anti- and pro-apoptotic proteins. We found that the anti-apoptotic BCL2 protein was repressed in CN1 mouse lungs after 14 days of DOX (Figure 2C). Induction of full-length, pro-apoptotic BCL2 family proteins BAK and BOK and the BH3-only proteins PUMA, BIK, BMF, and BIM, accompanied BCL2 repression (see Supplementary Figure 2A for unaltered BCL2 family proteins). Concurrently, cleaved forms of CASPASES 3 and 7, and the Caspase target PARP1 accumulated. We concluded that activated NOTCH1 induced alterations in multiple BCL2 family proteins to stimulate the intrinsic apoptotic cascade.

Both *Puma* (15) and *Bok* (16) are transcriptional targets of the p53 tumor suppressor. We reasoned that p53 induction might contribute to the apoptotic clearance of N1ICD-induced alveolar hyperplasia, but expression analysis of mRNAs encoding BCL2 family proteins altered by N1ICD showed a modest but statistically significant induction of *Bik* and *Bim*, but not *Puma* or *Bok* (Supplementary Figure 2B). In addition, neither p53 protein nor *trp53* mRNA was induced at day 14 of DOX treatment (Supplementary Figure 3A, B). We concluded that apoptotic signaling was engaged independent of p53 induction and that non-transcriptional regulatory mechanisms that are yet to be defined likely account for most of the observed alterations in BCL2 family proteins.

N1ICD-induced lung adenomas

We reasoned that over time genetic and/or epigenetic defects might accumulate in the lungs of CN1 mice, enabling cells to evade intrinsic tumor suppressive functions, such as apoptosis. Therefore, we monitored DOX-fed CN1 mice at different time-points for signs of tumorigenesis. Beginning as early as 8 months of age we observed that N1ICD overexpressing cells displayed an altered pattern of growth. Instead of growing as cell clusters (as in Figure 1E), some $N1ICD^+$ cells expanded laterally along the alveolar walls in a bronchioalveolar pattern (Figure 3A, B). Small adenomas could be found in each of the 8-month old CN1 mice (n=4 mice). These early tumors had bronchioalveolar patterning (Figure 3C) and appeared to have formed from the coalescence of $N1ICD^+$ cells (Figure 3D).

Eventually DOX-fed CN1 mice developed multiple adenomas with papillary histology (Figure 3E) and succumbed to their tumor burden at an average age of 15.1±2.2 months (n=11 mice). We did not find adenocarcinomas (size ≥ 5mm) in any of these mice. Only rare adenomas were found in CN1 mice not fed a DOX diet (average = 0.38±0.72 per mouse, n=16 mice).

We investigated the expression of markers of differentiated lung epithelial lineages in alveolar hyperplasia and the adenomas that arose in DOX fed CN1 mice. Alveolar hyperplasia in CN1 mice treated with DOX for 7 days was TTF-1$^+$ and SPC$^+$ (Supplementary Figure 4A–C), suggesting it may have arisen from type II pneumocytes where TTF-1 and SPC are co-expressed. Adenomas from CN1 mice were TTF-1$^+$ and CCSP$^-$ with scattered SPC$^+$ cells (Figure 3F–H). Therefore, both the expression of SPC and the anatomical location in which N1ICD$^+$ cells first arise suggest that N1ICD$^+$ adenomas may derive from type II cells.

The ARF/MDM2/p53 network in N1ICD-induced adenomas

We wondered what other factors contributed to the formation of lung adenomas in DOX treated CN1 mice. For example, in T-ALL, N1ICD suppresses the ARF/MDM2/p53 network (12). However, examination of the ARF/MDM2/p53 network in the lungs of CN1 mice demonstrated that p19^{ARF} was induced, not repressed, at both the protein and mRNA level when N1ICD was overexpressed (Supplementary Figure 3A, 5A). In addition, *Mdm2* was transcriptionally repressed in adenomas (Supplementary Figure 5B). Both findings are consistent with stabilization, not degradation, of p53, although no p53 accumulation was observed (Supplementary Figure 3A). Our data suggests that in the lung N1ICD does not inhibit p53 through repression of p19^{ARF}, a finding that contrasts with findings in T-ALL (12).

MYC and MYCL1 are induced in adenomas

We also examined the hypothesis that long-term formation of adenomas in CN1 mice could be mediated, at least in part, by MYC activity. Transcription from *MYC* is induced by activated NOTCH1 in T-ALL (17, 18) and in mammary tumors (19). We measured expression of MYC, MYCL1 and MYCN in lung protein extracts from CN1 mice treated with DOX. MYC and to a lesser extent MYCL1 were induced in the lungs of mice treated with DOX for 7 and 14 days (Figure 4A). The expression of both proteins was undetectable by day 30 of DOX treatment when hyperplasia had mostly resolved. However, expression of MYC and MYCL1 reemerged in adenomas from CN1 mice receiving long-term treatment with DOX (Figure 4A).

Next we measured the mRNA level of the *Myc* genes in the lungs and adenomas of CN1 mice. Although MYC and MYCL1 protein could be easily detected after just 7 days of DOX treatment, no changes in the transcription of any of the *Myc* genes was detected (Figure 4B). Adenomas, however, had upregulated transcription of both *Myc* and *MycL1*, but not *MycN*, a result that mirrored changes observed at the protein level. Therefore, transcriptional induction of both *Myc* and *Mycl1* could account for the presence of MYC and MYCL1 in adenomas, but altered post-transcriptional regulation likely underlies the upregulation of MYC and MYCL1 protein in N1ICD-induced alveolar hyperplasia. In any case, we concluded that MYC and MYCL1 expression reemerged in adenomas, presumably in response to selection that favored tumorigenesis.

MYC and N1ICD cooperate in lung tumorigenesis

To test whether sustained MYC activity could facilitate the formation of N1ICD-induced adenomas, we crossed CN1 mice to mice carrying a DOX-regulatable *MYC* transgene (13) (the M transgene) and created compound CN1M mice (schematic in Figure 5A). We found that mice overexpressing both N1ICD and MYC had dramatically decreased survival (Figure 5B) compared to mice overexpressing either N1ICD (CN1 mice) or MYC (CM mice) alone.

Tumorigenesis was always multi-focal in DOX fed CN1 mice (35.6±17.5 tumors visible on the pleural surface, n=11; Figure 5C, D), but the tumors in CN1 mice were always adenomas, never adenocarcinoma. In DOX fed CN1M mice we also observed multi-focal tumorigenesis (Figure 5E). However, not only were there more tumors in CN1M mice (113.3 ± 45.4 tumors visible on the pleural surface, n=10) but large adenocarcinomas, as well as adenomas, were found in each mouse. A significant proportion of CN1M mice harbored gross metastases (4/13, 30.8%) (Figure 5F–H). Metastatic cells were observed in enlarged lymph nodes, the liver and lining the walls of the thoracic cavity. TTF-1 staining confirmed the lung origin of distant metastases (Figure 5G, H).

We previously reported that a high percentage of CM mice succumb to lung adenocarcinomas (10). Usually, a single adenocarcinoma grew to occlude the parenchymal space (Figure 5I) before symptoms of respiratory distress were observed (1.3 ± 1.1 tumors per mouse, n=31). The data suggest that the combination of activated NOTCH1 and MYC induced a more aggressive lung tumor phenotype compared to mice expressing activated NOTCH1 or MYC alone.

N1ICD substitutes for activated RAS in lung tumors overexpressing MYC

Western analysis of tumor protein lysates suggested that even more of the 110 kDa N1ICD was present in CN1M adenocarcinomas than in CN1 adenomas (Figure 6A). MYC overexpression may therefore stabilize N1ICD, although a mechanism by which this might occur is not apparent. We concluded that both N1ICD and MYC were overexpressed in CN1M adenocarcinomas.

Like the levels of N1ICD, *Hes5* induction was highest in CN1M adenocarcinomas (Figure 6B), although the difference in expression compared to CN1 adenomas was not statistically significant. Other *Hes* and *Hey* genes were transcriptionally repressed in CN1M adenocarcinomas compared to CN1 adenomas (Supplementary Figure 6). This reinforces the supposition that *Hes5* is a target of N1ICD in the lung epithelium, while other *Hes* and *Hey* basic helix-loop-helix genes may not be.

Previously, we demonstrated that lung tumors from CM mice harbor mutations in *Kras* that cooperate with MYC in tumorigenesis (10). Crosstalk between NOTCH1 and RAS has been suggested to be important for transformation (20, 21) and in some mouse tumor models activated NOTCH1 cooperates with activated KRAS (22, 23). We hypothesized that cooperativity between N1ICD and MYC in lung tumorigenesis may require RAS activation and carried out a RAS activity assay on protein lysates of tumors from CN1, CN1M and CM mice (Figure 6C). No increase in RAS activity was seen in CN1 adenomas or CN1M adenocarcinomas. This suggests not only that RAS activation is not required for the formation of N1ICD-induced adenomas, but also that N1ICD can substitute for mutation of *Kras* in a cooperation with MYC that produces lung adenocarcinoma.

N1ICD and MYC have a synergistic effect on tumor cell proliferation

Acute overexpression of *MYC* induces apoptosis in a variety of tissues (24), including the lung (10). Compensatory genetic and/or epigenetic events are thought to counter the pro-apoptotic effects of MYC during tumorigenesis (25, 26). Given that overexpression of either N1ICD or MYC can elicit an anti-tumor response in the form of apoptosis, we wondered how cooperativity was achieved during lung tumorigenesis.

Tumors from CN1, CN1M and CM mice were immunostained for phospho-H3S10, a marker of cells in the mitotic phase of the cell cycle (Supplementary Figure 7A–C). We observed a significant increase in mitotic cells in CN1M adenocarcinomas compared to both CN1 adenomas (3.7 fold) and CM adenocarcinomas (3.3 fold) (Figure 6D). We observed

similar changes with immunostaining for Ki67 antigen (data not shown), which stains cells in all phases of the cell cycle. Therefore, the combination of N1ICD and MYC expression had a synergistic effect on tumor cell cycling.

We also observed an increase in TUNEL staining in adenocarcinomas from CN1M mice compared to CN1 adenomas (3.2 fold) and CM adenocarcinomas (2.8 fold) (Figure 6E, Supplementary Figure 7D–F). Therefore, the combination of N1ICD and MYC expression also augmented the induction of apoptosis. However, since the fold increase in phospho-H3S10^{+} cells was higher than the increase in TUNEL^{+} cells, the pro-proliferative effect of co-expressing activated NOTCH1 and MYC outcompeted apoptosis induction. Thus, synergistic activation of tumor cell cycling contributed to the cooperative effect of N1ICD and MYC on lung tumorigenesis.

Discussion

N1ICD induction of apoptosis in the alveolar epithelium

We used a DOX-inducible system to overexpress N1ICD in the lungs of adult mice. This resulted in the formation of lung adenomas. However, the initiation of adenomas required prolonged stimulation of the N1 transgene. Adenomas were first observed in 8 month-old CN1 mice that had been continuously fed a DOX diet. This chronology suggests that additional genetic/epigenetic events that cooperate with N1ICD overexpression must accumulate to enable N1ICD-induced tumorigenesis. The requirement for anti-apoptosis likely contributes to the observed latency.

The effect of activated NOTCH1 on apoptosis is context dependent. Activated NOTCH1 protects from apoptosis in some settings (27–29) but acts to induce apoptosis in others (30, 31). We found that in the mouse alveolar epithelium, acute activation of N1ICD overexpression resulted in a wave of proliferation and the formation of extensive hyperplasia, but the bulk of the alveolar hyperplasia was cleared from the lung periphery. The upregulation of multiple BH3-only proteins, Bak and Bok and repression of BCL2 all occurred, resulting in the activation of the intrinsic apoptotic cascade.

In this setting the induction of apoptosis may be tumor suppressive, effectively countering the mitogenic response to activated NOTCH1. Similar observations regarding the induction and apoptotic clearance of alveolar hyperplasia have been made in transgenic mice with lung-specific expression of MYC (10, 32), which also develop lung tumors following a prolonged latency period. This suggests that the acquisition of genetic/epigenetic events that provide anti-apoptosis may precede lung adenoma formation elicited by activated NOTCH1 and/or MYC.

Activated NOTCH1 and MYC cooperate in lung tumorigenesis

Based on the reemergence of MYC and MYCL1 expression in adenomas, we hypothesized that MYC activity could be important for the initiation of N1ICD-induced lung adenomas. We supposed that more adenomas would form if MYC activity were further supplemented through transgenic manipulation and developed mice that could overexpress both N1ICD and MYC coincidentally to test this supposition. These mice did have a significant increase in the number of lung tumors that were initiated, but the mice developed adenocarcinomas as well as adenomas. Some mice even harbored gross metastases. This suggests a robust cooperation between N1ICD and MYC in lung tumorigenesis.

Previously, we showed that activating mutations in *Kras* are present in *MYC* transgenic tumors, including CM lung adenocarcinomas (10). In this study, however, we observed that RAS is not activated in CN1M lung tumors. This suggests that activated NOTCH1 can

substitute for activated KRAS in tumorigenesis with MYC. It would be worthwhile to compare the frequency and overlap of *KRAS* mutation and activated NOTCH1 expression in human NSCLCs expressing MYC, as our data suggests *KRAS* mutation and activated NOTCH1 expression could be mutually exclusive.

Activated NOTCH1 and MYC synergistically activate tumor cell cycling

Despite the lack of progression of adenomas to adenocarcinoma in DOX-fed CN1 mice, the number of phospho-H3S10^{+} cells found in adenomas rivaled that found in adenocarcinomas from CM mice, which can grow to occlude entire lobes of the lung and metastasize (10). It would seem, therefore, that CN1 adenomas harbor a significant number of cells that can actively enter the cell cycle. Apoptotic cells, however, were also prevalent in CN1 adenomas. We suggest that apoptosis may limit the progression of CN1 adenomas to adenocarcinoma, although other means of tumor suppression might also contribute.

The supposition that apoptosis limited progression of adenomas to adenocarcinoma might seem paradoxical, since apoptosis was still prevalent in adenocarcinomas from DOX-fed CN1M mice. In fact, N1ICD and MYC co-expression induced a synergistic increase in apoptosis, as one might expect with two oncoproteins that can induce an apoptotic response. However, N1ICD and MYC co-expression also synergized in the induction of cell cycling. The fold-increase in mitotic cells was higher than the fold-increase in apoptotic cells. The observed synergy is in direct contrast to recent findings in a murine model of T-ALL, where supplementing the expression of MYC lent no additional advantage to malignant cells that overexpress N1ICD (33). Our findings suggest that small differences in the ratio of proliferating to apoptotic cells can have profound effects on lung tumor progression and survival, a supposition consistent with studies investigating the prognostic significance of apoptotic and proliferative indices in human NSCLC (34).

To our knowledge these are the first transgenic models to be reported in which lung tumors are directly induced by activated NOTCH1. The CN1 and CN1M models will be valuable for dissecting the genes and pathways that mediate the contribution of activated NOTCH1 to tumorigenesis in the lung. In addition, they may be valuable for the preclinical evaluation of therapeutics targeting either activated NOTCH1 or targets of NOTCH1 that are important for transformation.

Supplementary Material

Refer to Web version on PubMed Central for supplementary material.

Acknowledgments

We thank Luda Urisman for her help with the maintenance of the mouse colony and Rong Wang, Dean Sheppard and Jeffery Whitsett for transgenic mice.

Financial Support:

T.D.A. - Sandler Postdoctoral Research Fellowship

T.D.A., E.M.R., J.M.B. - G.W. Hooper Research Foundation

J.M.B. –N.I.H. Grant (CA009043)

References

1. Artavanis-Tsakonas S, Rand MD, Lake RJ. Notch signaling: cell fate control and signal integration in development. Science. 1999; 284:770–6. [PubMed: 10221902]

2. Kidd S, Lieber T, Young MW. Ligand-induced cleavage and regulation of nuclear entry of Notch in Drosophila melanogaster embryos. Genes Dev. 1998; 12:3728–40. [PubMed: 9851979]
3. Schroeter EH, Kisslinger JA, Kopan R. Notch-1 signalling requires ligand-induced proteolytic release of intracellular domain. Nature. 1998; 393:382–6. [PubMed: 9620803]
4. Jarriault S, Brou C, Logeat F, Schroeter EH, Kopan R, Israel A. Signalling downstream of activated mammalian Notch. Nature. 1995; 377:355–8. [PubMed: 7566092]
5. Ehebauer M, Hayward P, Martinez-Arias A. Notch signaling pathway. Sci STKE. 2006; 2006:cm7. [PubMed: 17148788]
6. Ellisen LW, Bird J, West DC, Soreng AL, Reynolds TC, Smith SD, et al. TAN-1, the human homolog of the Drosophila notch gene, is broken by chromosomal translocations in T lymphoblastic neoplasms. Cell. 1991; 66:649–61. [PubMed: 1831692]
7. Weng AP, Ferrando AA, Lee W, Morris JPt, Silverman LB, Sanchez-Irizarry C, et al. Activating mutations of NOTCH1 in human T cell acute lymphoblastic leukemia. Science. 2004; 306:269–71. [PubMed: 15472075]
8. Lee SH, Jeong EG, Yoo NJ. Mutational analysis of NOTCH1, 2, 3 and 4 genes in common solid cancers and acute leukemias. APMIS. 2007; 115:1357–63. [PubMed: 18184405]
9. Westhoff B, Colaluca IN, D'Ario G, Donzelli M, Tosoni D, Volorio S, et al. Alterations of the Notch pathway in lung cancer. Proc Natl Acad Sci U S A. 2009; 106:22293–8. [PubMed: 20007775]
10. Allen TD, Zhu C-Q, Jones KD, Yanagawa N, Tsao M-S, Bishop JM. Interaction between MYC and MCL1 in the genesis and outcome of non-small cell lung cancer. Cancer Research. 2011; 71:2212–21. [PubMed: 21406400]
11. Perl AK, Tichelaar JW, Whitsett JA. Conditional gene expression in the respiratory epithelium of the mouse. Transgenic Res. 2002; 11:21–9. [PubMed: 11874100]
12. Beverly LJ, Felsher DW, Capobianco AJ. Suppression of p53 by Notch in lymphomagenesis: implications for initiation and regression. Cancer Res. 2005; 65:7159–68. [PubMed: 16103066]
13. Felsher DW, Bishop JM. Reversible tumorigenesis by MYC in hematopoietic lineages. Mol Cell. 1999; 4:199–207. [PubMed: 10488335]
14. Nikitin AY, Alcaraz A, Anver MR, Bronson RT, Cardiff RD, Dixon D, et al. Classification of proliferative pulmonary lesions of the mouse: recommendations of the mouse models of human cancers consortium. Cancer Res. 2004; 64:2307–16. [PubMed: 15059877]
15. Nakano K, Vousden KH. PUMA, a novel proapoptotic gene, is induced by p53. Mol Cell. 2001; 7:683–94. [PubMed: 11463392]
16. Yakovlev AG, Di Giovanni S, Wang G, Liu W, Stoica B, Faden AI. BOK and NOXA are essential mediators of p53-dependent apoptosis. J Biol Chem. 2004; 279:28367–74. [PubMed: 15102863]
17. Weng AP, Millholland JM, Yashiro-Ohtani Y, Arcangeli ML, Lau A, Wai C, et al. c-Myc is an important direct target of Notch1 in T-cell acute lymphoblastic leukemia/lymphoma. Genes Dev. 2006; 20:2096–109. [PubMed: 16847353]
18. Sharma VM, Calvo JA, Draheim KM, Cunningham LA, Hermance N, Beverly L, et al. Notch1 contributes to mouse T-cell leukemia by directly inducing the expression of c-myc. Mol Cell Biol. 2006; 26:8022–31. [PubMed: 16954387]
19. Klinakis A, Szabolcs M, Politi K, Kiaris H, Artavanis-Tsakonas S, Efstratiadis A. Myc is a Notch1 transcriptional target and a requisite for Notch1-induced mammary tumorigenesis in mice. Proc Natl Acad Sci U S A. 2006; 103:9262–7. [PubMed: 16751266]
20. Fitzgerald K, Harrington A, Leder P. Ras pathway signals are required for notch-mediated oncogenesis. Oncogene. 2000; 19:4191–8. [PubMed: 10980592]
21. Weijzen S, Rizzo P, Braid M, Vaishnav R, Jonkheer SM, Zlobin A, et al. Activation of Notch-1 signaling maintains the neoplastic phenotype in human Ras-transformed cells. Nat Med. 2002; 8:979–86. [PubMed: 12185362]
22. Chiang MY, Xu L, Shestova O, Histen G, L'Heureux S, Romany C, et al. Leukemia-associated NOTCH1 alleles are weak tumor initiators but accelerate K-ras-initiated leukemia. J Clin Invest. 2008; 118:3181–94. [PubMed: 18677410]

23. De La OJ, Emerson LL, Goodman JL, Froebe SC, Illum BE, Curtis AB, et al. Notch and Kras reprogram pancreatic acinar cells to ductal intraepithelial neoplasia. Proc Natl Acad Sci U S A. 2008; 105:18907–12. [PubMed: 19028876]
24. Murphy DJ, Junttila MR, Pouyet L, Karnezis A, Shchors K, Bui DA, et al. Distinct thresholds govern Myc's biological output in vivo. Cancer Cell. 2008; 14:447–57. [PubMed: 19061836]
25. Meyer N, Kim SS, Penn LZ. The Oscar-worthy role of Myc in apoptosis. Semin Cancer Biol. 2006; 16:275–87. [PubMed: 16945552]
26. Hoffman B, Liebermann DA. Apoptotic signaling by c-MYC. Oncogene. 2008; 27:6462–72. [PubMed: 18955973]
27. Jehn BM, Bielke W, Pear WS, Osborne BA. Cutting edge: protective effects of notch-1 on TCR-induced apoptosis. J Immunol. 1999; 162:635–8. [PubMed: 9916679]
28. Choi YI, Jeon SH, Jang J, Han S, Kim JK, Chung H, et al. Notch1 confers a resistance to glucocorticoid-induced apoptosis on developing thymocytes by down-regulating SRG3 expression. Proc Natl Acad Sci U S A. 2001; 98:10267–72. [PubMed: 11504912]
29. Rangarajan A, Syal R, Selvarajah S, Chakrabarti O, Sarin A, Krishna S. Activated Notch1 signaling cooperates with papillomavirus oncogenes in transformation and generates resistance to apoptosis on matrix withdrawal through PKB/Akt. Virology. 2001; 286:23–30. [PubMed: 11448155]
30. Morimura T, Goitsuka R, Zhang Y, Saito I, Reth M, Kitamura D. Cell cycle arrest and apoptosis induced by Notch1 in B cells. J Biol Chem. 2000; 275:36523–31. [PubMed: 10967117]
31. Yang X, Klein R, Tian X, Cheng HT, Kopan R, Shen J. Notch activation induces apoptosis in neural progenitor cells through a p53-dependent pathway. Dev Biol. 2004; 269:81–94. [PubMed: 15081359]
32. Rapp UR, Korn C, Ceteci F, Karreman C, Luetkenhaus K, Serafin V, et al. MYC is a metastasis gene for non-small-cell lung cancer. PLoS One. 2009; 4:e6029. [PubMed: 19551151]
33. Demarest RM, Dahmane N, Capobianco AJ. Notch is oncogenic dominant in T-cell acute lymphoblastic leukemia. Blood. 2011; 117:2901–9. [PubMed: 21217079]
34. Tanaka F, Kawano Y, Li M, Takata T, Miyahara R, Yanagihara K, et al. Prognostic significance of apoptotic index in completely resected non-small-cell lung cancer. J Clin Oncol. 1999; 17:2728–36. [PubMed: 10561347]

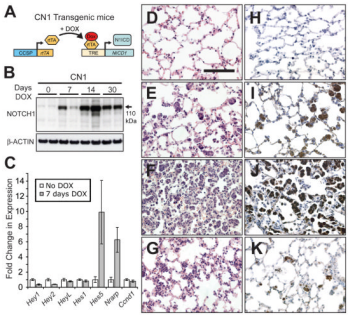

Figure 1.

Overexpression of N1ICD induces transient alveolar hyperplasia. **(A)** The C and N1 transgenes were used to direct N1ICD expression to lung epithelial cells with DOX treatment. **(B)** Western analysis of N1ICD expression in lung protein extracts following 0, 7, 14 and 30 days of DOX treatment. **(C)** Taqman® analysis of a subset of known NOTCH target genes using reverse transcribed lung RNA from CN1 mice either not treated with DOX or treated with DOX for 7 days (n≥3 mice, error bars are ± standard deviation). **(D–G)** H&E stained sections from CN1 lungs treated with DOX for 0 **(D)**, 7 **(E)**, 14 **(F)** and 30 **(G)** days. **(H–K)** Immunohistochemical staining for NOTCH1 in lung sections from CN1 mice treated with DOX for 0 **(H)**, 7 **(I)**, 14 **(J)** and 30 **(K)** days (bar in **D** = 0.1 mm, **D–K** same magnification).

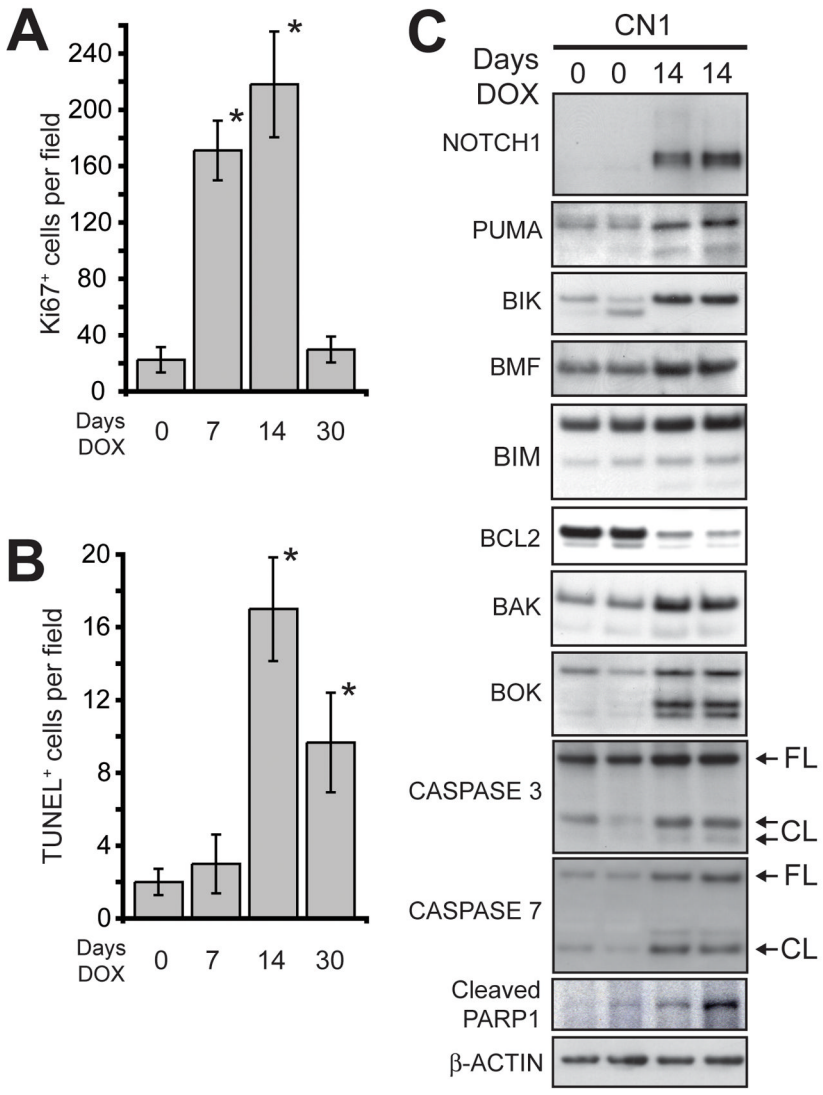

Figure 2.

Apoptosis contributes to the clearance of N1ICD overexpressing cells from the alveolar space. **(A)** Quantification of Ki67$^+$ cells in the lungs of DOX treated CN1 mice (n≥3 mice, error bars are ± standard deviation; * $p<0.01$ compared to day 0 by Student's t-test). **(B)** Quantification of TUNEL$^+$ cells in the lungs of DOX treated CN1 mice (n≥3 mice, error bars are ± standard deviation; * $p<0.003$ compared to day 0 by Student's t-test). **(C)** Western analysis of BCL2 family proteins, CASPASES 3 and 7 and PARP1 in the lungs of CN1 mice untreated and treated with DOX for 14 days (FL = full-length; CL= cleaved forms). β-ACTIN served as a loading control.

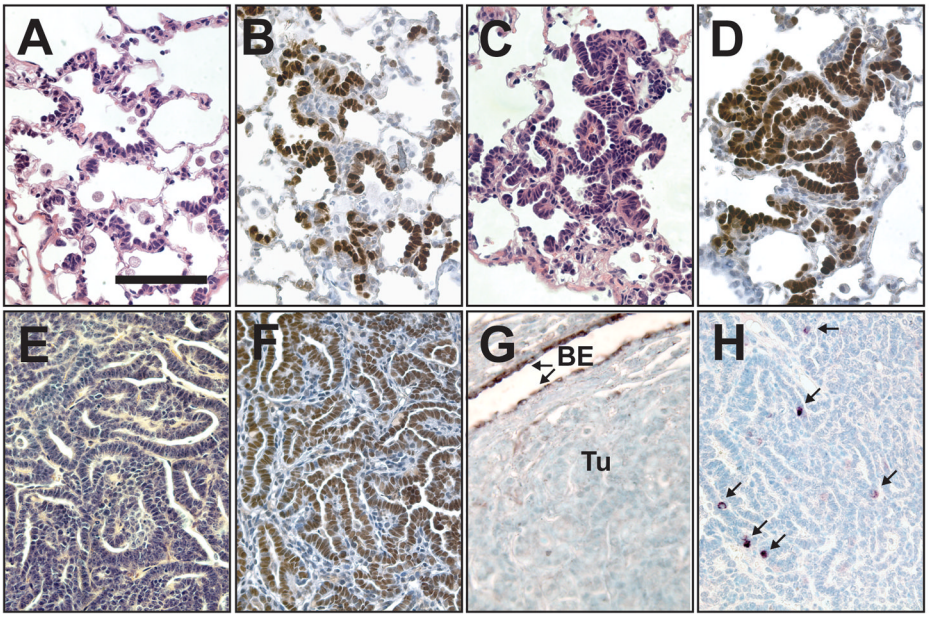

Figure 3.

Adenomas develop in the lungs of DOX treated CN1 mice. **(A–D)** Sections from CN1 mice maintained on DOX for 8 months. **(A)** H&E stained section showing organized growth along the alveolar walls. **(B)** Immunohistochemical staining for NOTCH1 showing that $N1ICD^{+}$ cells grow along the alveolar walls instead of in cell clusters. **(C)** H&E stained section showing an early adenoma. **(D)** Immunohistochemical staining of an early adenoma for NOTCH1. **(E–H)** Adenomas from CN1 mice maintained on DOX for > 1 year. **(E)** H&E stained section that shows the papillary patterning of a CN1 adenoma. Adenomas were $TTF\text{-}1^{+}$ **(F)**, but $CCSP^{-}$ (BE = bronchiolar epithelium; Tu = tumor) **(G)** with rare SPC^{+} cells (arrows) clearly discernable in immunohistochemically stained sections **(H)** (bar in **A** = 0.1 mm, **A–H** same magnification).

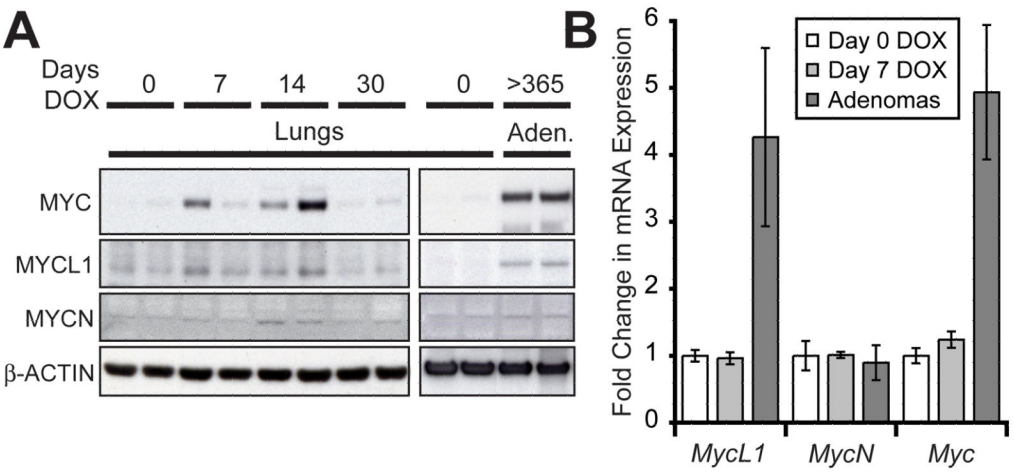

Figure 4.

MYC and MYCL1 are upregulated in N1ICD-induced adenomas. **(A)** Western analysis of MYC, MYCL1 and MYCN expression in the lungs of CN1 mice treated with DOX for 0, 7, 14 and 30 days and in adenomas from CN1 mice continuously fed a DOX diet until sacrifice (>1 year). β-ACTIN served as a loading control. **(B)** Taqman® analysis of *Myc* gene mRNA in the lungs of CN1 mice not treated with DOX, treated with DOX for 7 days and in adenomas from DOX fed mice (n≥3 mice, error bars are ± standard deviation). Gene expression was normalized to *β-Actin* expression.

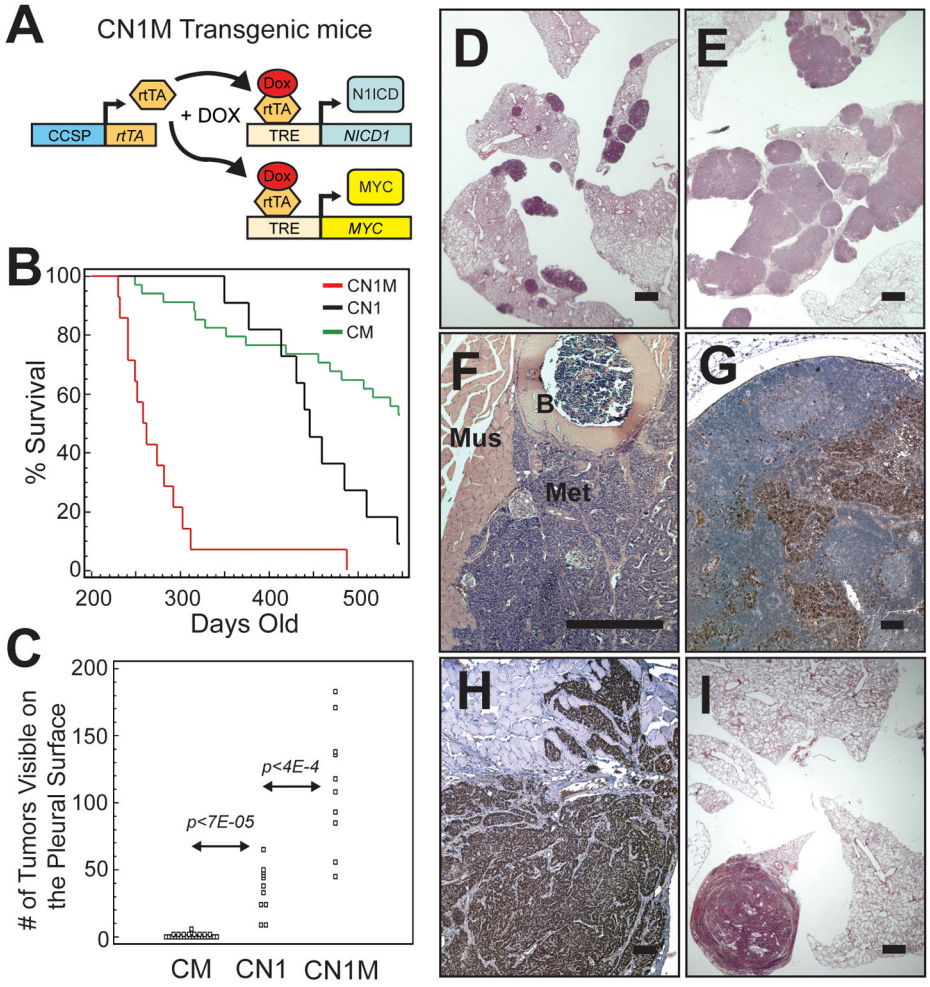

Figure 5.

N1ICD and MYC co-expression cooperates to induce lung adenocarcinoma. **(A)** Schematic of transgenes used for coincident overexpression of N1ICD and MYC. **(B)** Kaplan-Meier plot of DOX treated CM (n=34), CN1 (n=11) and CN1M (n=14) mice monitored for 18 months (*p<1E-4* by Logrank test for CN1M versus either CM or CN1). **(C)** Quantification of tumors visible on the pleural surface of transgenic mice (*p*-values calculated using Student's t-test). The cumulative numbers of tumors up until 18 months is displayed. **(D–F)** H&E stained sections from transgenic mice maintained on a DOX diet. **(D)** Lungs from a CN1 mouse with multiple adenomas. **(E)** Lungs from a CN1M mouse that developed multiple large adenocarcinomas. **(F)** Metastatic lesion growing on the wall of the thoracic cavity (B = bone; Mus = muscle; Met = metastases). **(G, H)** Immunohistochemical staining of metastases for the lung epithelial marker TTF-1. **(G)** TTF-1^+ cells (brown) in an enlarged lymph node. **(H)** TTF-1^+ cells that have invaded intercostal muscle of the ribcage. **(I)** H&E stained lung section from a DOX-fed CM mouse with a large adenocarcinoma (bars in **D**, **E**, **I** = 1 mm, **F**–**H** = 0.1 mm).

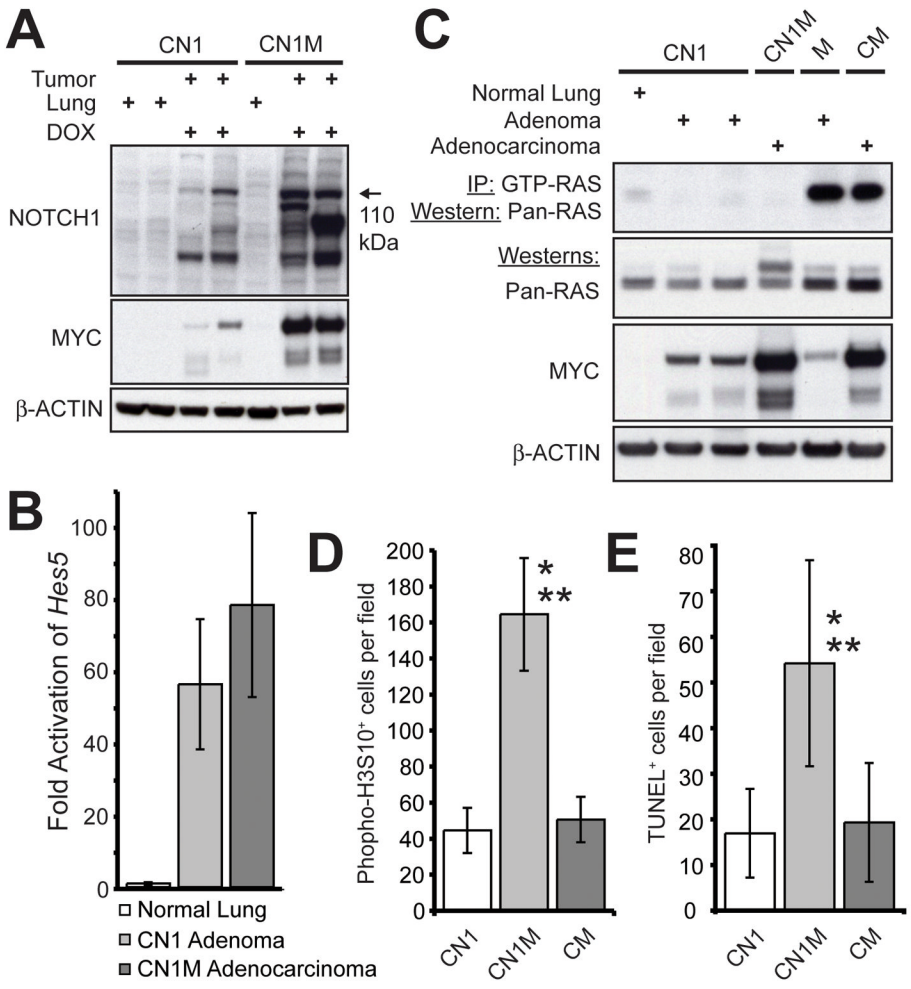

Figure 6.

Increased tumor cell cycling correlates with enhanced tumorigenesis in CN1M mice. **(A)** Western analysis of NOTCH1 and MYC expression in lungs and tumors from CN1 and CN1M transgenic mice. **(B)** Taqman® analysis comparing *Hes5* expression in the lungs of CN1 mice not treated with DOX and in tumors from DOX treated CN1 and CN1M mice. **(C)** RAS activity assay on protein lysates from normal lung and tumors from CN1 and CN1M transgenic mice. Tumor lysates from a spontaneous adenoma arising in a mouse carrying only the *MYC* transgene (no rtTA transgene present) and an adenocarcinoma from a CM mouse, both known to harbor an activating mutation in *Kras*, served as positive controls for RAS activity and RAS and MYC expression. β-ACTIN served as a loading control. **(D)** Quantification of phospho-H3S10$^+$ cells in tumors from DOX treated CN1 (n=12), CN1M (n=13) and CM (n=7) mice (* *p<8.2E-10* compared to CN1 adenomas; ** *p<1.7E-09* compared to CM adenocarcinomas; Student's T-test). **(E)** Quantification of TUNEL$^+$ cells in tumors from DOX treated CN1 (n=16), CN1M (n=15) and CM (n=13) mice (* *p<1.2E-5* compared to CN1 adenomas; ** *p<4.4E-05* compared to CM adenocarcinomas; Student's T-test).